

# Preparation and characterization of polyurethane–carbon nanotube composites

Hesheng Xia and Mo Song\*

Received 30th June 2005, Accepted 20th September 2005

First published as an Advance Article on the web 10th October 2005

DOI: 10.1039/b509038e

Well-dispersed and long-term stable carbon nanotubes/polyol dispersions were prepared by a mechanochemical approach with the aid of dispersing agent. Polyurethane (PU)–carbon nanotube nanocomposites were prepared by further *in situ* polymerization. Multi-walled carbon nanotubes (MWNT) can be dispersed individually. Fourier transform infrared (FTIR) spectra suggested that the addition of carbon nanotubes improved the degree of phase separation of polyurethane. Dynamic mechanical analysis (DMA) suggested that glass transition temperature ( $T_g$ ) of polyurethane decreased with increasing carbon nanotube content slightly. Tensile test suggested that MWNT is more helpful to improve the modulus than single-walled carbon nanotube (SWNT), which is more favourable to improve the elongation of polyurethane. The different reinforcing effects of MWNT and SWNT on PU were correlated to the shearing thinning exponent and the shape factor of carbon nanotubes in polyol dispersion. Raman shift of SWNTs can reflect the dispersion state of SWNT in polyol or in PU, and the interaction between polymer and SWNT. Both SWNT and MWNT can improve the thermal stability of polyurethane and thermal conductivity.

## Introduction

Polyurethane (PU) is one of the most versatile materials today. It is widely used in coatings, adhesives, thermoplastic elastomers and composite. PU generally consists of a soft segment which is a high molecular weight polyester or polyether macrodiol and a hard segment which is composed of diisocyanate and low molecular weight diol or diamine.<sup>1</sup> The most important feature of PU's structure is the microphase separation arising from the thermodynamic incompatibility of hard and soft segments. The modification of polyurethane mainly focuses on the mechanical properties and thermal stability. In general, there are two approaches: the first is to change the molecular structure of polyurethane by modification of its three basic building blocks: polyol, diisocyanate, and the chain extender. Polyol type plays a very important role for polyurethane properties. Compared to polycaprolactone polyol, polyether polyol such as polypropylene glycol (PPG) has a low tensile strength and elongation and low thermal stability, but its cost is low. The second is to introduce the inorganic filler into the polyurethane matrix. The disadvantages are that adding these inorganic fillers often worsens the fatigue behavior and reduces the elongation at break.

Carbon nanotubes (CNT) are ideal reinforcing fibers for composites because they have high aspect ratio, excellent mechanical strength, electrical and thermal conductivity and thermal stability.<sup>2–7</sup> Also, compared to conventional carbon fiber or glass fiber, carbon-nanotube-filled polymer composites are easily processed due to its small diameter. These materials can keep the polymer matrix properties (elasticity, strength and modulus) with the additional functionality of exceptionally

high electrical and thermal conductivity. Novel carbon nanotube–polymer composites open opportunities for new multi-functional materials with broad commercial and defense applications. The big challenges encountered in making such a composite are the uniform dispersion of carbon nanotubes in polymer matrix without agglomerates and entanglements, and the improved nanotubes–resin interface adhesion.

Since Ajayan *et al.* first reported a polymer–carbon nanotube composite in 1994,<sup>8</sup> a lot of papers on this kind of advanced materials can be found. The polymer matrix includes poly(methyl methacrylate),<sup>9–13</sup> polystyrene,<sup>14–18</sup> epoxy,<sup>19–23</sup> polypropylene,<sup>24–28</sup> polyethylene,<sup>29–33</sup> nylon<sup>34–37</sup> *etc.* It is surprising that only a few reports involved with polyurethane–carbon nanotube composites can be found.<sup>38–41</sup> This is possibly due to the difficulty in achieving a good dispersion of carbon nanotubes in polyurethane matrix and thus deterioration of polyurethane properties. This paper is aimed at the preparation and characterization of polyurethane–carbon nanotube composite elastomer. The carbon nanotubes were dispersed into polyol by mechanochemical milling with the aid of dispersing agent. And polyurethane–carbon nanotube nanocomposite were prepared by further *in situ* polymerization. This study will endeavor to solve the dispersion problem of carbon nanotubes in highly viscous polyol liquid media and study the relationship between the structure and properties of PU–CNT composites. The interaction between polyurethane and carbon nanotubes, thermal stability and thermal conductivity were also examined.

## Experimental

### Materials

MWNTs and SWNTs were provided by Chengdu Institute of Organic Chemistry, Chinese Academy of Sciences. The

*Institute of Polymer Technology and Materials Engineering, Loughborough University, Loughborough, Leicestershire, UK LE11 3TU. E-mail: m.song@lboro.ac.uk; Fax: (+44) 1509 223949; Tel: (+44) 1509 223160*

as-grown MWNTs and SMNTs were produced by CCVD, in which  $\text{CH}_4$  or  $\text{C}_2\text{H}_2$  were converted into CNTs at 700 and 1000 °C in the presence of a Ni–La<sub>2</sub>O<sub>3</sub> catalyst. The diameter of MWNT and SWNT was at 8–15 nm, and 1–2 nm, respectively. The products were washed with concentrated hydrochloric acid to remove the catalyst and the carrier of catalyst, and then were purified with concentrated HNO<sub>3</sub> to remove the amorphous carbon particles. Polyether polyol (Luprane 2090, molecular weight: 6000; functionality: 3), was provided by Elastogran UK, Ltd. 4,4'-Methylenebis(phenyl isocyanate) (MDI) was provided by Hyperlast Ltd., UK. 1,4-Butanediol was purchased from the Aldrich Chemical Company. The catalyst Dabco-33LV was obtained from Air Products and Chemicals. The dispersing agent BYK-985, BYK-9076, and BYK-9077 were provided by Blagden Specialty Chemicals Ltd., England.

### Preparation of PU–carbon nanotube composites

(1) Preparation of the stable polyol–CNT dispersions: Typically, 194 g of polyol, 4 g of MWNTs or SWNTs, and 2 g of dispersion agent BYK 9077 were mixed at 80 °C by ball milling for 72 h. As a control experiment, a mixture with the same recipe was blended and stirred at 600 rpm for 4 h at 80 °C.

(2) Preparation of PU–CNT composites: PU–CNT composites at a hard segment content of 26% were prepared. The –NCO/OH ratio was kept at 1.1 : 1 for every sample. Typically, 20 g of polyol–CNT dispersion was blended with 0.89 g of 1,4-butanediol, 5.93 g of MDI and 0.03 g of Dabco-33LV at room temperature for 2 min and was vacuum-degassed for 3–5 min to remove the bubbles. Then the viscous prepolymer was poured into an O-ring metal mold and cured at 50 °C for 24 h and 80 °C for one week to obtain PU–CNT composites.

### Characterization

The viscosity of the liquid polyol–clay mixture was determined by a Haake VT500 instrument with a Haake K20 circulator. The shear rate was changed from 4.45 s<sup>-1</sup> to 444.6 s<sup>-1</sup>.

Tensile tests were carried out using a Hounsfield test machine at room temperature. The specimens were stretched until break at a crosshead rate of 500 mm min<sup>-1</sup>. The stress–strain curves were recorded. The tensile strength, elongation, and modulus at 50%, 100%, 200% and 300% strain were the average values of five specimens.

Transmission electron microscopy (TEM) analysis was conducted on a JEOL 2100 FX equipment. The ultrathin cryo-sectioning of PU–CNT samples was conducted in Birmingham University.

Fourier transform infra-red (FTIR) spectra of the samples in KBr pellets were recorded on a Mattson 3000 FTIR spectrometer by using the ATR mode. The spectra were collected from 4000 to 400 cm<sup>-1</sup>, with a 4 cm<sup>-1</sup> resolution over 120 scans.

Dynamic mechanical analysis (DMA) was performed on a Dynamic Mechanical Thermal Analyser Mk II. The samples were heated from –80 °C to 200 °C at a heating rate of 3 °C min<sup>-1</sup>.

Thermogravimetric analysis (TGA) was performed on a Hi-Res Modulated TGA 2950 instrument. The samples were

heated from room temperature to 600 °C at a heating rate of 10 °C min<sup>-1</sup>.

Raman spectra were recorded on a Jobin Yvon Horiba high-resolution LabRam 800 Raman microscope system, which contains an optical microscope adapted to a double grating spectrograph and a CCD array detect. The laser excitation was provided by a Spectra-Physics model 127 helium–neon laser operating at 35 mW of 633 nm output. The laser power at the sample was ~8 mW and was focused to ~10 μm. Spectra were recorded by scanning the 50–3000 cm<sup>-1</sup> region with a total acquisition time of 3 min. Wavenumber calibration was carried out using the 520.5 cm<sup>-1</sup> line of a silicon wafer. A spectra resolution of ~1 cm<sup>-1</sup> was used.

The measurement of thermal conductivity was performed using a modulated differential scanning calorimeter (TA Instruments 2920 MDSC Calorimeter) according to ASTM E1952-98 standard method. The heating rate was 5 °C min<sup>-1</sup>, and the degree of modulation was ±1 °C every 80 s for the measurement of specific heat capacity.

## Results and discussion

### The dispersion of carbon nanotubes in polyol and polyurethane

The dispersion of carbon nanotubes in viscous polyol liquid is the key issue to prepare polyurethane–carbon nanotubes composite. Due to the incompatibility of carbon nanotubes and polyol, it is impossible to attain the good dispersion of carbon nanotubes in polyol by direct mixing. In this paper, we tried to utilize the ball milling method to break the agglomerate of carbon nanotubes and reach the good dispersion. Fig. 1 shows the dispersion stability of carbon nanotubes in polyol after ball milling 72 h and stirring at 600 rpm for 6 h at 80 °C. The dispersions were deposited for one month. It is clear that ball milling has a much better effect on the dispersion stability of CNT in polyol than conventional stirring. During a milling process, the moving balls impact on the CNT aggregates, the kinetic energy within the CNT aggregates is partially transformed into mechanical stresses to disintegrate the materials. Ball milling can provide pulverization and dispersion functions on carbon nanotubes in polyol. However, it is difficult to obtain a long-term stable polyol–CNT dispersion only by ball milling, because CNT will re-aggregate with time. So, it is necessary to use the dispersing agent to adjust the interaction between polyol and CNTs and make it stable for a long time. Three dispersion agents marked BYK-985, BYK-9076 and BYK-9077 were selected. The mixture of

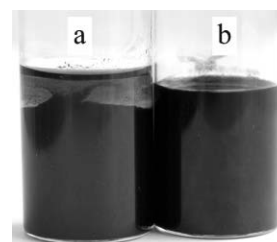
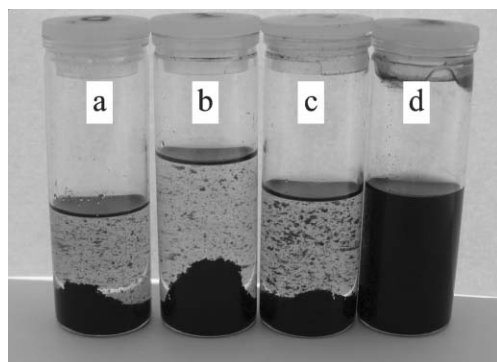


Fig. 1 Effect of different mixing method (a: stirring; b: ball milling) on the stability of polyol/CNT dispersions.



**Fig. 2** Effect of different dispersing agents (a: no dispersing agent; b: BYK-985; c: BYK-9076; d: BYK-9077) on the stability of polyol/CNT dispersions.

polyol, CNTs and dispersion agent was milled and then the formed dispersion was centrifuged for 1 h at 4000 rpm. The result is shown in Fig. 2 and it can be noted that the effect of dispersion agent BYK-9077 on the dispersion stability of CNTs in polyol was much better than the others. Dispersion agent BYK-9077 is a high molecular weight copolymer with some affinic groups to carbon nanotubes. It is assumed that the dispersing agent with one end anchored onto the CNT surface is solvated in polyol and the adsorbed polymer layer on the surface of CNT provides a steric stabilization function. So, by combining the mechanochemical effect of ball milling and steric stabilization function of dispersion agent, a good dispersion of carbon nanotubes in polyol matrix can be attained. This method can be extended to other systems such as epoxy. To further characterize the dispersion of CNT in polyurethane, the soft samples were cryo-sectioned, and then were observed by TEM. The dispersion of MWNT and SWNT is shown in Fig. 3. It is clear that MWNTs were well dispersed in the polyurethane matrix. The MWNT has a diameter of 10–20 nm, same as the original MWNTs, suggesting it is dispersed in the polyurethane individually. However, SWNT still existed in an aggregate state at a submicron scale. It is difficult to attain the individual dispersion of SWNT in organic media, and in most cases SWNT is existed in an aggregate state due to van der Waals attraction.<sup>23</sup>

## FTIR

Phase separation is an important factor for PU physical properties. The degree of phase separation in segmented PU can be estimated following the work of Cooper *et al.*<sup>42</sup> The hydrogen bonding was constituted by the NH groups being as proton donor and the oxygen in carbonyls of the hard segment and in ethers of the soft segment as proton acceptors. The formation of hydrogen bonding by  $\text{-C=O}$  group can be determined by examining the peak position at  $\sim 1705\text{ cm}^{-1}$  for hydrogen bonded  $\text{-C=O}$  and at  $\sim 1728\text{ cm}^{-1}$  for free  $\text{-C=O}$ . By measuring the peak intensity ratio of these two carbonyl groups, it is possible to give an estimate of the degree of hydrogen bonding. The hydrogen bonding index,  $R$ , can be defined as the ratio of absorption peak  $A_{1709}/A_{1731}$ . In association with the change of absorption peaks of NH groups, the degree of phase separation and the degree of phase

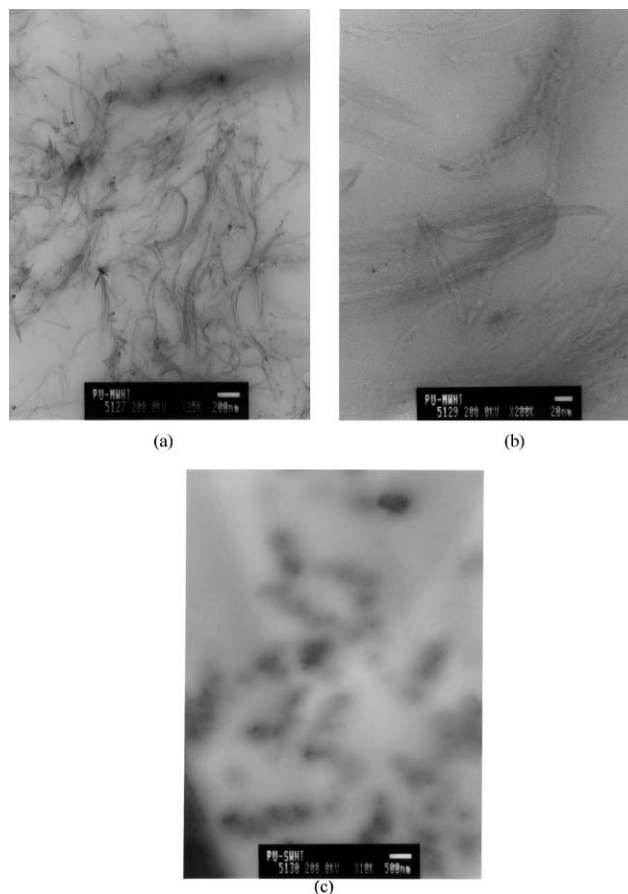


**Fig. 3** TEM photographs of polyurethane/1 wt% MWNT (a, b) and polyurethane/1 wt% SWNT (c) nanocomposites.

mixing of segmented PU can be calculated. In addition, the hydrogen bonding index,  $R$ , can be obtained from a base-line approach method:  $R = C_{\text{bonded}}\epsilon_{\text{bonded}}/C_{\text{free}}\epsilon_{\text{free}} = A_{1709}/A_{1731}$ , where  $C$  is the concentration and  $\epsilon$  is the respective extinction coefficient of bonded and free carbonyl groups. The degree of phase separation (DPS) can be obtained by the equation:  $\text{DPS} = C_{\text{bonded}}/(C_{\text{bonded}} + C_{\text{free}})$  or  $\text{DPS} = R/(R + 1)$ .<sup>43</sup> Here the ratio of  $\epsilon_{\text{bonded}}/\epsilon_{\text{free}}$  is taken as 1 according to Cooper.<sup>42</sup> Figs. 4 and 5 show FTIR spectra of PU–MWNT composites and PU–SWNT composite, respectively. The peak was fitted by Microcal Origin software and the area of peak at  $\sim 1730\text{ cm}^{-1}$  and  $1709\text{ cm}^{-1}$  was calculated to evaluate the hydrogen bonding index,  $R$ , and the degree of phase separation (DPS). The results were shown in Table 1. It is clear that with increasing the MWNT or SWNT content, the hydrogen bonding index increased and thus the degree of phase separation increased. Compared to MWNT system, phase separation was improved more significantly in SWNT system. These results maybe explain why SWNT–PU composite have a higher elongation and tensile strength compared to MWNT–PU composite.

## Dynamical mechanical analysis (DMA)

The storage modulus  $E'$  and damping factor  $\tan \delta$  of PU and PU–SWNT composites as a function of temperature were

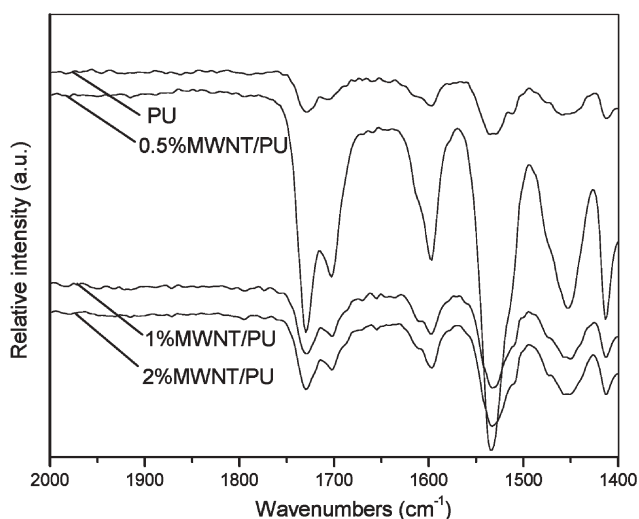


Fig. 4 FTIR spectra of PU and PU–MWNT composites.

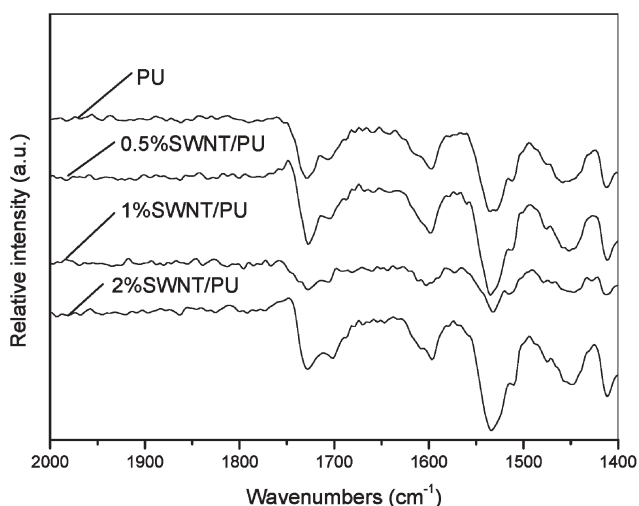


Fig. 5 FTIR spectra of PU and PU–SWNT composites.

**Table 1** Hydrogen bonding index  $R$  and degree of phase separation (DPS) for PU–MWNT and PU–SWNT composites

| CNT content | $R$  |      | DPS  |      |
|-------------|------|------|------|------|
|             | MWNT | SWNT | MWNT | SWNT |
| 0%          | 0.86 | 0.86 | 0.46 | 0.46 |
| 0.5%        | 0.99 | 1.54 | 0.50 | 0.61 |
| 1%          | 1.08 | 1.55 | 0.52 | 0.61 |
| 2%          | 1.09 | 2.11 | 0.52 | 0.68 |

shown in Figs. 6 and 7, respectively. It can be noted that  $E'$  increased with increasing the SWNT content in PU nearby room temperature. The  $\tan \delta$  peak is associated with the soft segment glass transition temperature ( $T_g$ ). It is clear that the introduction of SWNT resulted in a slight decrease in  $T_g$  and damping capacity. Two effects must be considered in this system, one is that well-dispersed SWNTs will restrict the molecular motion, and this will lead to an increase in  $T_g$ . On the other hand, the increase in microphase separation with the introduction of SWNT as suggested by FTIR results will lead

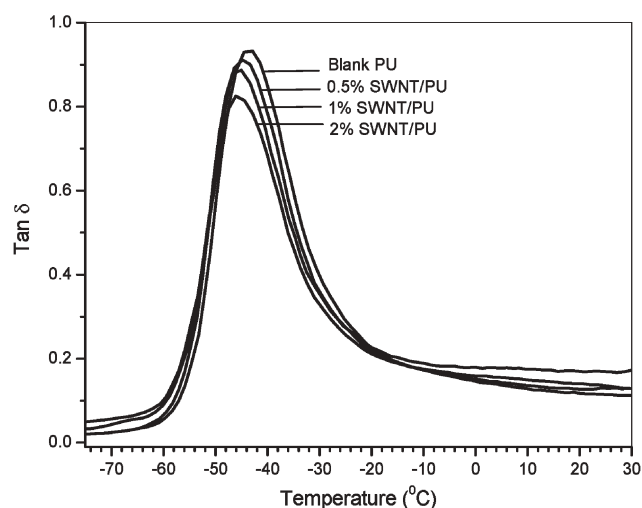


Fig. 6 Damping factor ( $\tan \delta$ ) of polyurethane and polyurethane–SWNT nanocomposites as a function of temperature.

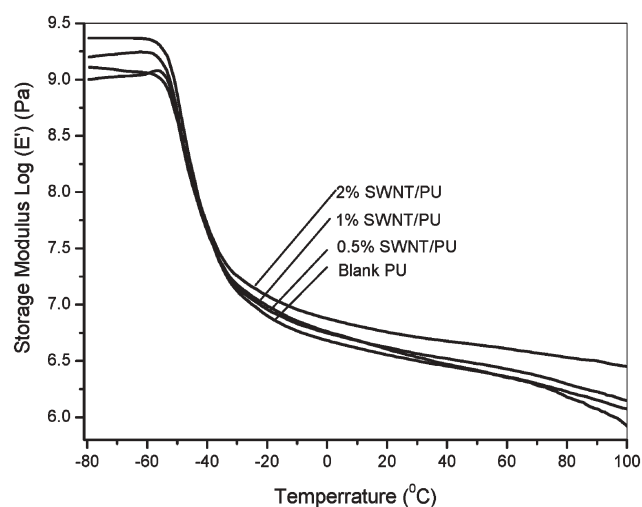
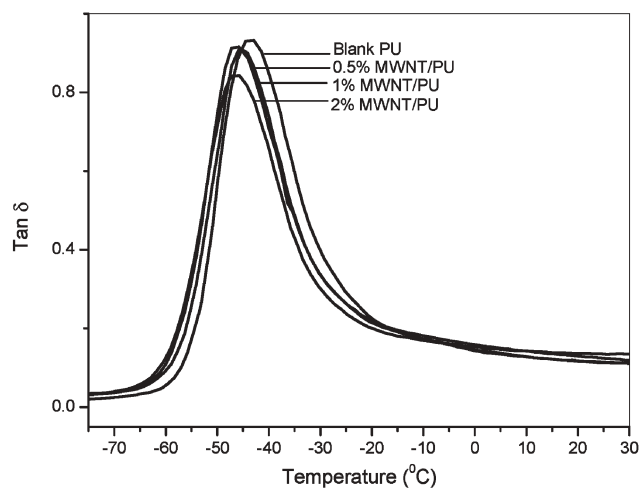


Fig. 7 Storage modulus ( $E'$ ) of polyurethane and polyurethane–SWNT nanocomposites as a function of temperature.

to a decrease in  $T_g$  because there are less hard segments present in the soft phase hindering the motion of soft segment. This result suggests that the latter plays a more important role in  $T_g$  shift. As shown in Figs. 8 and 9, MWNT series have some similar results with SWNT series. With an increase of MWNT content,  $E'$  increased at room temperature and  $T_g$  decreased slightly.

## Raman

Raman is a very important method to determine the structure change of polymer–carbon nanotubes composite.<sup>44</sup> Raman has been used to determine the diameter of nanotubes, chirality, type, the diameter distribution of nanotubes bundles, and the aggregation state of nanotubes. Raman shift can provide an insight on the dispersion of carbon nanotubes and interaction between polymer and carbon nanotubes.<sup>45,46</sup> A prominent feature is radial breathing mode (RBM) in the 160–300  $\text{cm}^{-1}$  region, associated with a symmetric movement of all carbon



**Fig. 8** Damping factor ( $\tan \delta$ ) of polyurethane and polyurethane-MWNT nanocomposites as a function of temperature.

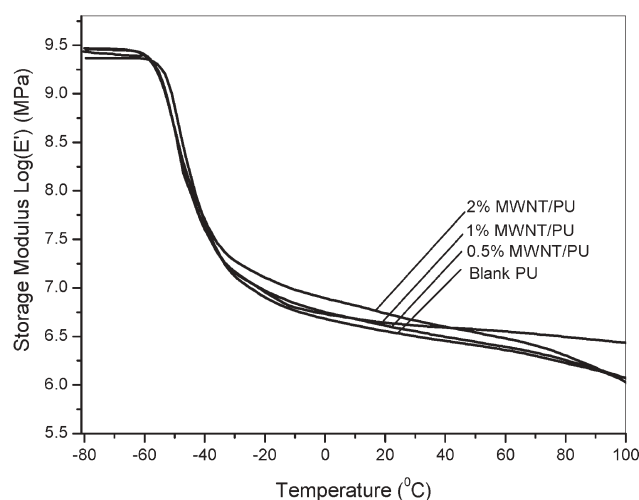


**Fig. 9** Storage modulus ( $E'$ ) of polyurethane and polyurethane-MWNT nanocomposites as a function of temperature.

atoms in the radial direction. The D-mode or D Raman band (the disordered band is located between  $1330\text{--}1360\text{ cm}^{-1}$  when excited with a visible laser) is expected to be observed in MWNTs. However when it is observed in SWNTs, one assumes that it is due to defects in the tubes. The G-mode (tangential mode) corresponds to the stretching mode in the graphite plane, and this mode is located around  $1580\text{ cm}^{-1}$ . The G' or D\* band is the second-order overtone of D band. The locations of D and D\* Raman bands of CNTs depend linearly on the laser excitation energy and the dispersion of nanotubes.

Raman spectra of SWNT, SWNT-polyol dispersion, PU and SWNT-PU composites are shown in Fig. 10. When SWNT was mixed with polyol, no new Raman peak appeared compared to SWNT. A lot of strong peaks appeared in the Raman spectra of blank polyurethane. It is interesting that with the addition of SWNT, Raman peaks of PU weaken and finally disappear at 2% SWNTs, which indicates SWNT has a strong effect on the PU Raman spectra. The reason is not clear. Due to the strong peak of SWNT in polyurethane and different peak position of SWNT and polyurethane, Raman is

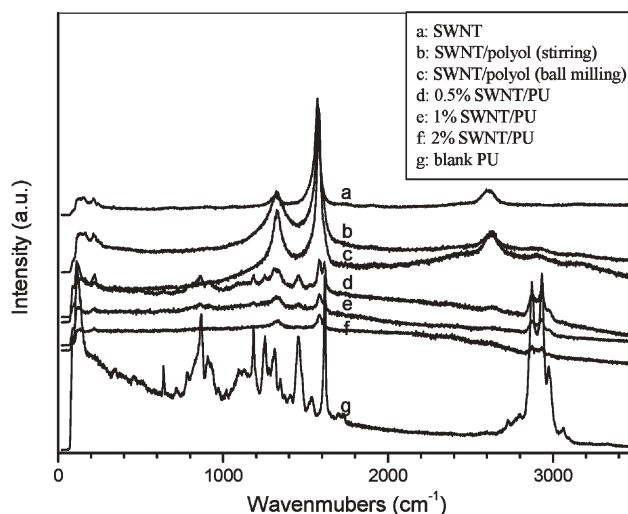


**Fig. 10** Raman spectra of SWNT, SWNT-polyol dispersion, PU and SWNT-PU composites.

an important tool to characterize the interaction between polyurethane and carbon nanotubes, especially the effect of polymer on the carbon nanotubes. The detailed Raman RBM shift and G-band shift are shown in Figs. 11 and 12. Table 2 lists the shifts of the RBM mode and G, G' and B-band. It is clear that a shift to a large wavenumber can be observed in four modes. The shift is relative to the dispersion state of SWNTs in the matrix and the chemical environment surrounding the SWNTs. When SWNT was in a state of bad dispersion (stirred polyol-SWNT sample), a slight shift can be observed due to the effect of polyol medium. A larger shift occurred in the well-dispersed polyol-SWNT dispersion by ball milling and SWNT-PU composites. So, it can be concluded that the better dispersion of SWNT in polyol and polyurethane can lead to the larger shift of the characteristic peaks.

Raman spectra of MWNT series are shown in Fig. 13. For MWNT, two characteristic peaks can be observed, and the intensity is weak. Like the SWNT-PU series, with the addition

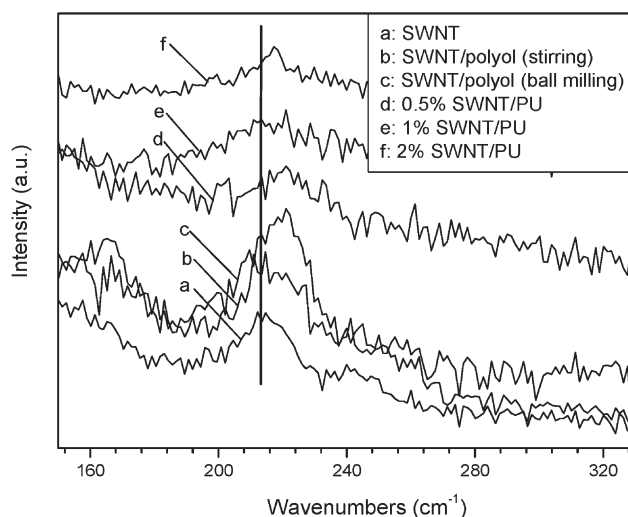


**Fig. 11** Raman radial breathing mode of SWNT, SWNT-polyol dispersion and SWNT-PU composites.

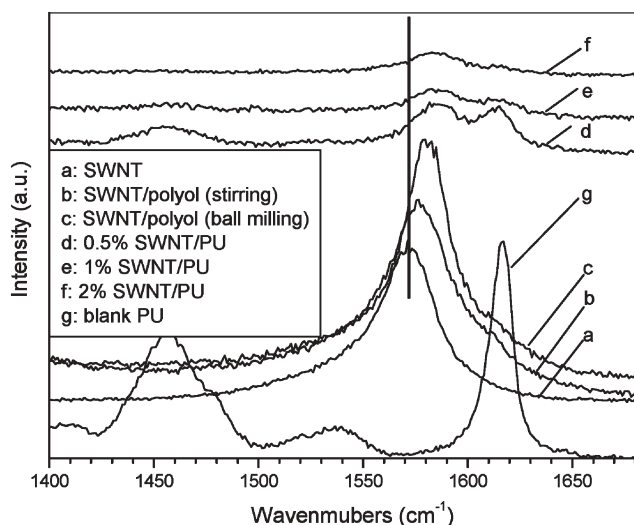


**Fig. 12** Raman G-mode of SWNT, SWNT-polyol dispersion and SWNT-PU composites.

**Table 2** Raman shift in SWNT, SWNT-polyol and SWNT-polyurethane composites

|                            | G' band | G band | D band | RBM band |
|----------------------------|---------|--------|--------|----------|
| SWNT                       | 2615    | 1571   | 1316   | 212      |
| SWNT-polyol (stirring)     | 2625    | 1576   | 1322   | 214      |
| SWNT-polyol (ball milling) | 2628    | 1581   | 1327   | 221      |
| 0.5% SWNT                  | 2630    | 1585   | 1325   | 222      |
| 1% SWNT                    | 2628    | 1583   | 1333   | 221      |
| 2% SWNT                    | 2628    | 1584   | 1332   | 219      |

of MWNT, Raman peaks of PU weaken and finally disappear. There are strong PU characteristic peaks present nearby the characteristic peak of MWNT. Unlike SWNT, it is difficult to determine the effect of polyurethane on MWNTs due to the peak overlay.

### Rheological behavior of polyol-carbon nanotubes dispersions

Polyol-CNT dispersions play an important role in polyurethane preparation and the final properties of PU-CNT nanocomposites. The rheological behavior of polyol-MWNT and polyol-SWNT dispersions was investigated. The variation of viscosity of polyol-CNTs dispersions with shearing rate was determined at 20 °C, 40 °C, and 60 °C, respectively. Fig. 14 shows the typical curves of viscosity vs shearing rate at different temperatures for 1% SWNT-polyol dispersion. The data can be fitted very well with the Herschel-Bulkley model.<sup>47</sup> The viscosity ( $\eta$ ) of Herschel-Bulkley suspensions can be calculated according to eqn. (1):<sup>48</sup>

$$\eta = \tau_0 / \dot{\gamma} + k \dot{\gamma}^{n-1} \quad (1)$$

$\dot{\gamma}$  is the shear rate,  $k$  and  $\tau_0$  are constants,  $n$  is the flow behavior index. When  $n > 1$ , the fluid exhibits a shear-thickening behaviour; when  $n = 1$ , the fluid exhibits a Bingham plastic behavior; when  $n < 1$ , the fluid exhibits a shear-thinning behavior. The  $n$  value can denote the shearing-thinning exponent. When  $\tau_0$  is equal to zero, eqn. (1) is equal to a power law model. It is believed that the  $n$ ,  $k$ ,  $\tau_0$  values are

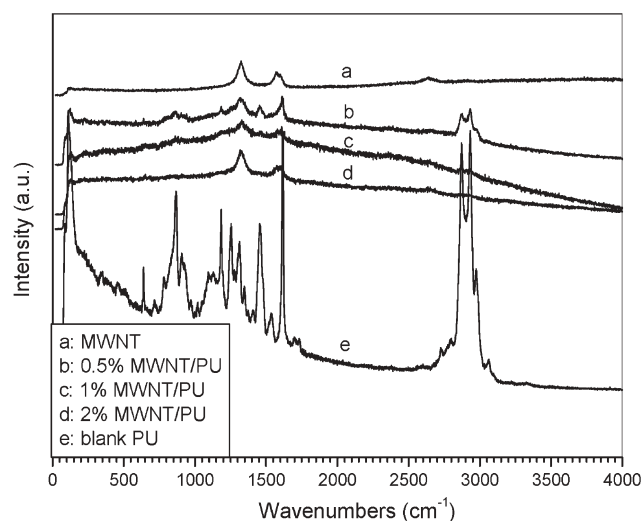


**Fig. 13** Raman spectra of MWNT, MWNT-polyol dispersion, PU and MWNT-PU composites.

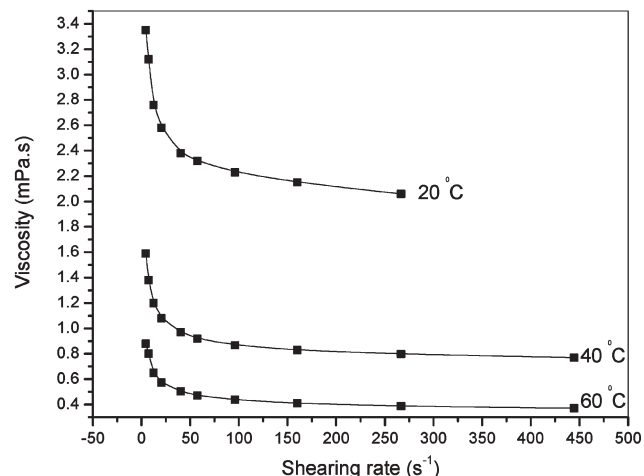


**Fig. 14** Variation of viscosity with shearing rate at different temperature for 1% SWNT-polyol dispersion.

related to the dispersion state of carbon nanotubes. Carbon nanotubes are one kind of filler with a high aspect ratio. If the carbon nanotubes were in a state of good dispersion, high shearing will make the nanotubes align with the flow direction, and thus make the viscosity decrease. If the carbon nanotubes existed in an aggregation state, shearing thinning behaviour will be very weak. The better the dispersion of carbon nanotubes, the lower the shearing thinning exponent  $n$ . In Fig. 14, the scatter points are the experimental data, the solid lines are the fitted curves according to the Herschel-Bulkley model. The related rheological data were listed in Table 3. For MWNT and SWNT series, with increasing the concentration of carbon nanotubes, the shearing thinning exponent decreased, which means a more significant shearing thinning behaviour. Also, on increasing the temperature, the shearing thinning behaviour decreases, which means a better dispersion state of carbon nanotubes at a higher temperature. These are common features for SWNT-polyol and MWNT-polyol. An interesting phenomenon is that the viscosity for MWNT-polyol dispersions is

**Table 3** The viscosity at low shearing rate of  $4.45 \text{ s}^{-1}$  ( $\eta_L$ ) and high shear rate of  $159.8 \text{ s}^{-1}$  ( $\eta_H$ ) and shear thinning parameter  $n$ 

| T/°C | Concentration (%) | $\eta_L/\text{mPa s}$ |      | $\eta_H/\text{mPa s}$ |       | $n$   |       |
|------|-------------------|-----------------------|------|-----------------------|-------|-------|-------|
|      |                   | MWNT                  | SWNT | MWNT                  | SWNT  | MWNT  | SWNT  |
| 20   | 0                 | 1.59                  | 1.59 | 1.58                  | 1.58  | 1.000 | 1.000 |
|      | 0.5               | 2.31                  | 1.96 | 1.99                  | 1.79  | 0.968 | 0.975 |
|      | 1                 | 3.32                  | 3.35 | 2.44                  | 2.15  | 0.908 | 0.928 |
|      | 2                 | 12.50                 | 8.00 | 4.45                  | 2.95  | 0.751 | 0.830 |
| 40   | 0                 | 0.59                  | 0.59 | 0.59                  | 0.59  | 0.999 | 0.999 |
|      | 0.5               | 0.95                  | 0.92 | 0.75                  | 0.69  | 0.959 | 0.950 |
|      | 1                 | 1.67                  | 1.59 | 1.02                  | 0.83  | 0.894 | 0.916 |
|      | 2                 | 6.8                   | 3.95 | 2.06                  | 1.21  | 0.759 | 0.786 |
| 60   | 0                 | 0.30                  | 0.30 | 0.27                  | 0.27  | 0.981 | 0.981 |
|      | 0.5               | 0.46                  | 0.53 | 0.35                  | 0.34  | 0.933 | 0.943 |
|      | 1                 | 1.11                  | 0.88 | 0.50                  | 0.41  | 0.866 | 0.874 |
|      | 2                 | 5.47                  | 2.85 | 1.09                  | 0.656 | 0.771 | 0.746 |

higher than that for SWNT–polyol and shearing thinning behaviour for MWNT–polyol is more apparent since they have a lower  $n$  value. If we consider the different dimension of SWNTs and MWNTs, one can infer that the SWNTs dispersion should have a more significant shearing thinning behaviour due to its high aspect ratio. However, this is not the case. The probable reason is that an individual dispersion of SWNTs is difficult to attain. In most cases, the SWNTs still existed in an aggregate state, especially in an organic medium.<sup>23</sup> Further, we analyze the variation of viscosity of MWNT–polyol and SWNT–polyol dispersions at a shear rate of  $444.6 \text{ s}^{-1}$  and at  $60^\circ\text{C}$  with CNTs concentration. The data is shown in Fig. 15. The viscosity can be fitted very well with eqn. (2):<sup>49</sup>

$$\eta = \eta_0(1 + 0.67fC + 1.62f^2C^2) \quad (2)$$

$f$  is the shape factor, or the aspect ratio, *i.e.*, the ratio of the longest to shortest diameter of particles.  $\eta_0$  is the viscosity when CNTs concentration is zero.  $C$  is the concentration of CNTs. The fitted parameters  $\eta_0$  and  $f$  value are listed in Table 4. Clearly, MWNTs have a much bigger  $f$  value than SWNTs. This result can be related to our TEM observation. The  $f$  value is dependent on the CNT morphology in polyol. A better dispersion of CNT leads to a high aspect ratio and thus a bigger  $f$  value. The rheological data including the viscosity, the fitted shearing thinning exponent and shape factor gave an insight into the different reinforcing effects of MWNTs and SWNTs as suggested below. In contrast to SWNT–PU composite, the more reinforcing effect, *i.e.*, higher modulus for MWNT–PU composite should relate to higher viscosity, more obvious shearing thinning behaviour of polyol–MWNT dispersion and higher shape factor  $f$  value of MWNT in polyol dispersion.

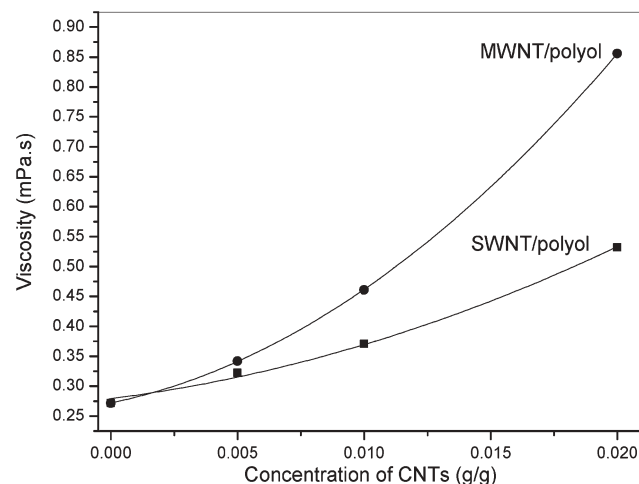
### Mechanical properties

The tensile properties of MWNT–PU and SWNT–PU composites were determined. The results were shown in Table 5. From Table 5, it can be noted that the introduction of MWNTs can improve the modulus and the tensile strength. At a 2% MWNT content, the modulus at 50% strain was improved by  $\sim 38\%$ . But the elongation at break kept nearly unchanged for MWNTs series. The introduction of SWNTs can improve the elongation at break and tensile strength. At a

2% SWNT content, the tensile strength and elongation was improved by  $\sim 60\%$  and  $\sim 42\%$  respectively. However, the modulus was improved slightly in contrast to MWNT series. It is clear that MWNT and SWNT have different effects on the mechanical properties of polyurethane. MWNT is more helpful to the improvement of modulus, whilst SWNT for elongation and tensile strength. The difference in reinforce effect could be related to the rheological behaviour of MWNT and SWNT in polyol. As mentioned above, the shape factor  $f$  of MWNT in polyol is bigger and the shearing thinning behaviour of MWNT is more apparent compared to that of SWNT.

### Thermogravimetric analysis (TGA)

The degradation of polyurethane is a complicated process. In general, the thermal degradation of polyurethane occurs in two

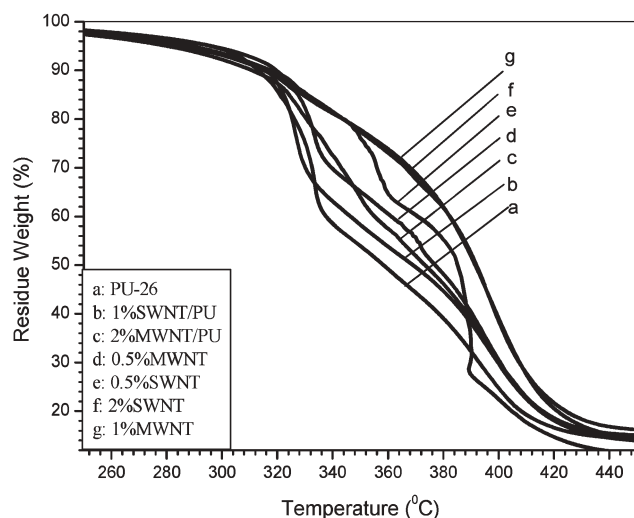
**Fig. 15** Variation of viscosity of MWNT/polyol and SWNT–polyol dispersions at a shear rate of  $444.6 \text{ s}^{-1}$  and at  $60^\circ\text{C}$  with CNTs concentration.**Table 4** The fitted  $\eta_0$  and  $f$  value for polyol–SWNT and polyol–MWNT dispersions

|             | $\eta_0$ | $f$   |
|-------------|----------|-------|
| Polyol–SWNT | 0.279    | 28.52 |
| Polyol–MWNT | 0.272    | 48.14 |

**Table 5** Tensile properties of PU–MWNT and PU–SWNT composites

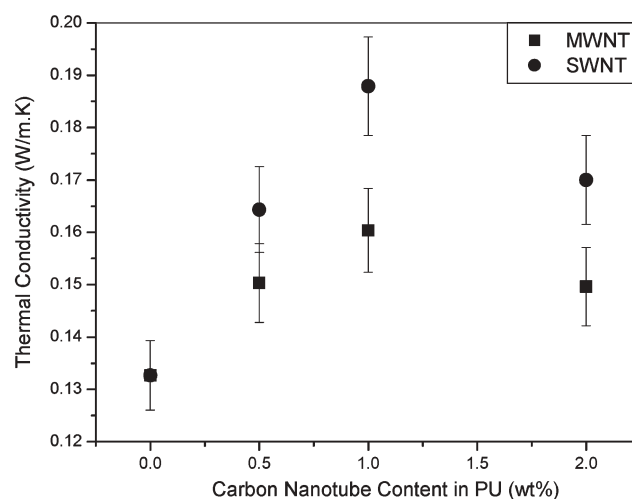
| Sample    | Stress MPa | Strain% | Modulus/MPa, 50% | Modulus/MPa, 100% | Modulus/MPa, 200% | Modulus/MPa, 300% |
|-----------|------------|---------|------------------|-------------------|-------------------|-------------------|
| PU-26     | 5.85       | 452     | 1.17             | 1.73              | 2.77              | 3.93              |
| 0.5% MWNT | 5.68       | 404     | 1.32             | 1.92              | 3.05              | 4.31              |
| 1% MWNT   | 7.12       | 489     | 1.39             | 2.02              | 3.20              | 4.49              |
| 2% MWNT   | 6.66       | 405     | 1.61             | 2.34              | 3.70              | 5.13              |
| 0.5% SWNT | 7.53       | 578     | 1.20             | 1.71              | 2.74              | 3.83              |
| 1% SWNT   | 8.54       | 639     | 1.14             | 1.70              | 2.70              | 3.79              |
| 2% SWNT   | 9.11       | 638     | 1.31             | 1.87              | 3.01              | 4.22              |

stages: the initial degradation stage I is primarily the decomposition of the hard segment, which involves the dissociation of urethane to the original polyol and isocyanate, which then form a primary amine, alkene and carbon dioxide. Stage I is influenced by the hard segment content. The consequent stage II proceeds by the depolycondensation and polyol degradation mechanisms, and is affected by the soft segment content.<sup>50,51</sup> In general, the temperature at the maximum mass loss rate in the TG curve corresponds to the accepted thermal decomposition temperature of the composite. The TGA results were shown in Fig. 16. The first degradation of blank polyurethane occurred at  $\sim 332$  °C and the second degradation at 393 °C. The incorporation of MWNT and SWNT didn't improve the first degradation temperature, but did improve the second degradation temperature. This indicates that carbon nanotubes may preferably interact with the soft segment in polyurethane structure. There are no significant differences between SWNT and MWNT series. At 1 wt% of SWNT or MWNT loading, the second degradation temperature is delayed by  $\sim 5$  K. There are three reasons to be responsible for the improvement in thermal stability: (1) the uniformly dispersed carbon nanotubes presumably provided thermo-oxidative stability to the polymers in the vicinity of the tube surfaces; (2) the enhanced thermal conductivity of the composite can facilitate heat transport and thus increase its thermal stability;<sup>52</sup> (3) like fullerene ( $C_{60}$ ), carbon nanotubes possibly can lead to the formation and stabilization of the CNT-bonded macroradicals.<sup>53</sup>

**Fig. 16** TGA curves for polyurethane and polyurethane–carbon nanotubes composites.

### Thermal conductivity

Thermal conductivity of SWNT at room temperature is as high as  $\sim 6600$   $W\ m^{-1}\ K^{-1}$ ,<sup>54</sup> and the experimental value of  $3000$   $W\ m^{-1}\ K^{-1}$  for MWNT at room temperature has also been reported.<sup>55</sup> Carbon nanotubes might be used as fillers to enhance the thermal conductivity of polymer materials. In this study, the thermal conductivity of PU and PU–carbon nanotubes were determined by MDSC. The results are shown in Fig. 17. It is clear that incorporation of carbon nanotubes enhances the thermal conductivity. At 1% carbon nanotube loading, the thermal conductivity of PU–MWNT and PU–SWNT was improved by  $\sim 21\%$  and  $\sim 42\%$  compared to blank polyurethane. SWNT has a better effect on the improvement of thermal conductivity compared to MWNT. Our conclusion agrees with the recent reports.<sup>56,57</sup> The limitation of CNT on improvement of thermal conductivity is still not very clear. Keblinski *et al.*<sup>52</sup> think the increase in thermal conductivity appears rather limited by a large thermal resistance across the nanotube–matrix interface even for the case with ultrahigh intrinsic thermal conductivity and aspect ratio of the carbon nanotubes embedded. Interfacial resistance happens when the frequencies are different, and the heat energy has a difficult time taking the leap from one element to the next. Padgett *et al.*<sup>58</sup> attribute this to a reduction in phonon scattering length rather than changes in the vibration frequencies of the carbon atoms in the nanotubes.

**Fig. 17** Thermal conductivity of MWNT–polyurethane and SWNT–polyurethane composites at 27 °C.

## Conclusion

The good dispersion of carbon nanotubes in polyol was realized by mechanochemical approach with the assistance of specific dispersing agent. Furthermore, the polyurethane-carbon nanotubes composites were prepared by *in situ* polymerization. The different effects of MWNT and SWNT on polyurethane were disclosed. FTIR results suggested that incorporation of SWNT leads to a higher phase separation degree of polyurethane than MWNT. The glass transition temperature of polyurethane decreased slightly with increasing carbon nanotube content. Tensile test suggested that MWNT is more helpful to improve the modulus than SWNT, which is more favourable to improve the elongation of polyurethane. The difference in reinforcing effect of MWNT and SWNT on PU was correlated to the shearing thinning exponent of polyol-CNT dispersion and the shape factor of carbon nanotubes in polyol. Raman shift of SWNTs can reflect the dispersion state of SWNT in polyol or PU, and the interaction between polymer and SWNT. Both SWNT and MWNT can improve the thermal stability and thermal conductivity of polyurethane.

## References

- 1 C. Hepburn, *Polyurethane Elastomer*, Applied Science Publishers, London, 1982.
- 2 P. Calvert, *Nature*, 1999, **399**, 210.
- 3 M. S. P. Shaffer and A. H. Windle, *Adv. Mater.*, 1999, **11**, 937.
- 4 H. Xia, Q. Wang and G. Qiu, *Chem. Mater.*, 2003, **15**, 3879.
- 5 T. Kashiwagi, E. Grulke, J. Hilding, R. Awad, W. Harris and J. Douglas, *Macromol. Rapid Commun.*, 2002, **23**, 761.
- 6 S. H. Qin, D. Q. Qin, W. T. Ford, D. E. Resasco and J. E. Herrera, *J. Am. Chem. Soc.*, 2004, **126**, 170.
- 7 R. Andrews, D. Jacques, M. Minot and T. Rantell, *Macromol. Mater. Eng.*, 2002, **7**, 395.
- 8 P. M. Ajayan, O. Stephan, C. Colliex and D. Tranth, *Science*, 1994, **265**, 1212.
- 9 Z. J. Jia, Z. Y. Wang, C. L. Xu, J. Liang, B. Q. Wei, D. H. Wu and S. W. Zhu, *Mater. Sci. Eng., A*, 1999, **271**, 395.
- 10 Z. Jin, K. P. Pramoda, G. Xu and S. H. Goh, *Chem. Phys. Lett.*, 2001, **337**, 43.
- 11 S. J. Park, M. S. Cho, S. T. Lim, H. J. Cho and M. S. Jhon, *Macromol. Rapid Commun.*, 2003, **24**, 1070.
- 12 J. H. Sung, H. S. Kim, H. J. Jin, H. J. Choi and I. J. Chin, *Macromolecules*, 2004, **37**, 9899.
- 13 R. E. Gorga and R. E. Cohen, *J. Polym. Sci., Polym. Phys. Ed.*, 2004, **42**, 2690.
- 14 D. Qian, E. C. Dickey, R. Andrews and T. Rantell, *Appl. Phys. Lett.*, 2000, **76**, 2868.
- 15 C. A. Mitchell, J. L. Bahr, S. Arepalli, J. M. Tour and R. Krishnamoorti, *Macromolecules*, 2002, **35**, 8825.
- 16 K. Liao and S. Li, *Appl. Phys. Lett.*, 2001, **79**, 4225.
- 17 S. O. Obare, N. R. Jana and C. J. Murphy, *Nano Lett.*, 2001, **1**, 601.
- 18 P. C. P. Watts, W. K. Hsu, G. Z. Chen, D. J. Fray, H. W. Kroto and D. R. M. Walton, *J. Mater. Chem.*, 2001, **11**, 2482.
- 19 L. S. Schadler, S. C. Giannaris and P. M. Ajayan, *Appl. Phys. Lett.*, 1998, **73**, 3842.
- 20 J. Sandler, M. S. P. Shaffer, T. Prasse, W. Bauhofer, K. Schulte and A. H. Windle, *Polymer*, 1999, **40**, 5967.
- 21 X. J. Xu, M. M. Thwe, C. Shearwood and K. Liao, *Appl. Phys. Lett.*, 2002, **81**, 2833.
- 22 S. Barrau, P. Demont, C. Maraval, A. Bernes and C. Lacabanne, *Macromol. Rapid Commun.*, 2005, **26**, 390.
- 23 X. D. Li, H. S. Gao, W. A. Scrivens, D. L. Fei, X. Y. Xu, M. A. Sutton, A. P. Reynolds and M. L. Myrick, *Nanotechnology*, 2004, **15**, 1416.
- 24 B. P. Grady, F. Pompeo, R. L. Shambaugh and D. E. Resasco, *J. Phys. Chem. B*, 2002, **106**, 5852.
- 25 A. R. Bhattacharyya, T. V. Sreekumar, T. Liu, S. Kumar, L. M. Ericson, R. H. Hauge and R. E. Smalley, *Polymer*, 2003, **44**, 2373.
- 26 E. Assouline, A. Lustiger, A. H. Barber, C. A. Cooper, E. Klein, E. Wachtel and H. D. Wagner, *J. Polym. Sci., Poly. Phys. Ed.*, 2003, **41**, 520.
- 27 L. Valentini, J. Biagiotti, J. M. Kenny and S. J. Santucci, *J. Appl. Polym. Sci.*, 2003, **87**, 708.
- 28 H. S. Xia, Q. Wang, K. S. Li and G. J. Hu, *J. Appl. Polym. Sci.*, 2004, **93**, 378.
- 29 S. L. Ruan, P. Gao, X. G. Yang and T. X. Yu, *Polymer*, 2003, **44**, 5643.
- 30 W. Z. Tang, M. H. Santare and S. G. Advani, *Carbon*, 2003, **41**, 2779.
- 31 Y. Z. Bin, M. Kitanaka, D. Zhu and M. Matsuo, *Macromolecules*, 2003, **36**, 6213.
- 32 K. Mylvaganam and L. C. Zhang, *J. Phys. Chem. B*, 2004, **108**, 5217.
- 33 P. Potschke, A. R. Bhattacharyya and A. Janke, *Polymer*, 2003, **44**, 8061.
- 34 J. B. Gao, M. E. Itkis, A. P. Yu, E. Bekyarova, B. Zhao and R. C. Haddon, *J. Am. Chem. Soc.*, 2005, **127**, 3847.
- 35 M. Endo, S. Koyama, Y. Matsuda, T. Hayashi and Y. A. Kim, *Nano Lett.*, 2005, **5**, 101.
- 36 T. X. Liu, I. Y. Phang, L. Shen, S. Y. Chow and W. D. Zhang, *Macromolecules*, 2004, **37**, 7214.
- 37 W. D. Zhang, L. Shen, I. Y. Phang and T. X. Liu, *Macromolecules*, 2004, **37**, 256.
- 38 H. Koerner, G. Price, N. A. Pearce, M. Alexander and R. A. Vaia, *Nat. Mater.*, 2004, **3**, 115.
- 39 H. Koerner, W. Liu, M. Alexander, P. Mirau, H. Dowty and R. A. Vaia, *Polymer*, 2005, **46**, 4405.
- 40 J. W. Cho, J. W. Kim, Y. C. Jung and N. S. Goo, *Macromol. Rapid Commun.*, 2005, **26**, 412.
- 41 R. Sen, B. Zhao, D. Perea, M. E. Itkis, H. Hu, J. Love, E. Bekyarova and R. C. Haddon, *Nano Lett.*, 2004, **4**, 459.
- 42 R. W. Seymour, G. M. Ester and S. L. Cooper, *Macromolecules*, 1970, **3**, 579.
- 43 T. K. Chen, Y. I. Tien and K. H. Wei, *Polymer*, 2000, **41**, 1345.
- 44 Q. Zhao and H. D. Wagner, *Philos. Trans. R. Soc. London, Ser. A*, 2004, **362**, 2407.
- 45 M. Lucas and R. J. Young, *Compos. Sci. Technol.*, 2004, **64**, 2297.
- 46 D. A. Heller, P. W. Barone, J. P. Swanson, R. M. Mayrhofer and M. S. Strano, *J. Phys. Chem. B*, 2004, **108**, 6905.
- 47 W. H. Herschel and R. Bulkeley, *Proc. Am. Test. Mater.*, 1926, **26**, 621.
- 48 G. Matijašić and A. Glasnović, *Chem. Biochem. Eng. Q.*, 2002, **16**, 165.
- 49 L. H. Cohan, *Proceedings of the Second Rubber Technology Conference*, Heffers & Sons, Ltd., Cambridge, UK, 1948, p. 365.
- 50 F. S. Chuang, W. C. Tsen and Y. C. Shu, *Polym. Degrad. Stab.*, 2004, **84**, 69.
- 51 Z. S. Petrović, Z. Zavargo, J. H. Flynn and W. J. Macknight, *J. Appl. Polym. Sci.*, 1994, **51**, 1087.
- 52 S. T. Huxtable, D. G. Cahill, S. Shenogin, L. Xue, R. Ozisik, P. Barone, M. L. Usrey, M. S. Strano, G. Siddons, M. Shim and P. Keblinski, *Nat. Mater.*, 2003, **2**, 731.
- 53 B. M. Ginzburg, L. A. Shibaev, V. L. Ugolkov and V. P. J. Bulatov, *Macromol. Sci.*, 2003, **B42**, 139.
- 54 S. Berber, Y. K. Kwon and D. Tománek, *Phys. Rev. Lett.*, 2000, **84**, 4613.
- 55 J. P. Smalla, L. Shib and P. Kim, *Solid State Commun.*, 2003, **127**, 181.
- 56 T. Kashiwagi, E. Grulke, J. Hilding, K. Groth, R. Harris, K. Butler, J. Shields, S. Kharchenko and J. Douglas, *Polymer*, 2004, **45**, 4227.
- 57 Y. S. Song and J. R. Youn, *Carbon*, 2005, **43**, 1378.
- 58 C. W. Padgett and D. W. Brenner, *Nano Lett.*, 2004, **4**, 1051.